Real Compton Scattering via Color Dipoles

B.Z. Kopeliovich,[1,2,*] Ivan Schmidt,[1,†] and M. Siddikov[1,‡]

[1] *Departamento de Física, Centro de Estudios Subatómicos, y Centro Científico - Tecnológico de Valparaíso, Universidad Técnica Federico Santa María, Casilla 110-V, Valparaíso, Chile*

[2] *Joint Institute for Nuclear Research, Dubna, Russia*

We study photoabsorption reaction and real Compton scattering (RCS) within the color dipole model. We rely on a photon wave function derived in the instanton vacuum model, and on the energy dependent phenomenological elastic dipole amplitude. Data for the photoabsorption cross section at high energies agree with our parameter free calculations. We also provide predictions for the differential RCS cross section. Although no data for small angle Compton scattering are available so far, this process can be measured in ultra-peripheral hadronic and nuclear collisions at the LHC.

arXiv:0906.5589v2 [hep-ph] 24 Aug 2009

I. INTRODUCTION

Compton scattering, $\gamma+p\to\gamma+p$, and related photoabsorption reaction, have been a subject of intensive theoretical and experimental investigation [1, 2, 3, 4, 5, 6, 7, 8, 9, 10, 11, 12, 13, 14, 15]. While in the case of deeply-virtual Compton scattering (DVCS), where the initial photon is highly-virtual, the QCD factorization is proven [5, 7, 8] and the amplitude can be expressed in terms of the generalized parton distributions (GPD) [1, 2, 3, 4, 5, 6, 7, 8, 9, 10, 11, 12, 13, 14, 15], in the case of real Compton scattering (RCS) the available theoretical tools are rather undeveloped.

On the one hand, as it has been shown in [16, 17], for large momentum transfer $\Delta_\perp$ it is possible to factorize the RCS amplitude [18, 19] and express it in terms of the distribution amplitudes of the proton. On the other hand, it is possible to express the amplitude of the process via the minus 1st-moment of GPDs at zero skewedness [5, 20, 21].

The traditional sources of quasi-real and virtual photons, the electron beams, with very high collisions energies are expected to be available in near future. The new projects of LHeC [22, 23] and EIC [24, 25] are currently under intensive discussion. Besides the electron beams, one can also use beams of charged hadrons. Provided that the transverse overlap of the colliding hadrons is small, i.e. the transverse distance b between the colliding centers is larger than the sizes of the colliding particles, $b>R_1+R_2$, the electromagnetic interaction between colliding particles becomes the dominant mechanism. Such processes called ultra-peripheral collisions (UPC) can be studied in pp, pA and AA collisions. In particular, one can access RCS in the reaction

$$A_1+A_2\ \to A_1+\gamma+A_2. \tag{1}$$

The typical virtualities $\left\langle Q^2_{\gamma^*}\right\rangle$ of the intermediate photon γ^* are controlled by the formfactors of the colliding particles, and are small:

$$\left\langle Q^2_{\gamma^*}\right\rangle \lesssim \frac{3}{R_A^2}\sim\frac{0.1\,GeV^2}{A^{2/3}}. \tag{2}$$

Thus, $\left\langle Q^2_{\gamma^*}\right\rangle$ is of the order of the soft hadronic scale, so the intermediate photon can be treated as a free Weizsäcker-Williams one, i.e. the amplitude of the process (1) can be described in terms of RCS.

These processes at the LHC will allow to study RCS at very high energies. The possibility of observation of such processes experimentally has been demonstrated by the STAR [26, 27, 28] and PHENIX [29] experiments at RHIC. It is expected that at LHC photon-proton collisions at energies up to $\sqrt{s_{\gamma p}}\lesssim 8\times10^3$ GeV can be observed [30]. In this paper we concentrate on RCS on a proton target. Nuclear effects will be discussed elsewhere.

In what follows we employ the color dipole approach introduced in [31, 32]. The central objects of the model are the dipole scattering amplitude, $\mathcal{A}(s,\beta,\vec{r})$ and the light-cone quark distribution functions of the photon. While pQCD predicts the dipole amplitude only for small-size dipoles, several successful phenomenological parameterizations for the large-size dipoles are known. Relying on the photon wave function evaluated in the instanton vacuum model [33], which is valid for any Q^2, one can extend the applicability of the model to the case of the processes with real photons [34]. In this paper we are going to consider the real photoabsorption, $\gamma+p\to X$, and the RCS.

*Electronic address: Boris.Kopeliovich@usm.cl

†Electronic address: Ivan.Schmidt@usm.cl

‡Electronic address: Marat.Siddikov@usm.cl

II. COLOR DIPOLE MODEL

The color dipole model is valid only at sufficiently high energies, where the dominant contribution to the Compton amplitude comes from gluonic exchanges. Then the general expression for the Compton amplitude in the color dipole model has the form,

$$\mathcal{A}_{\mu\nu}\left(s,\Delta\right)\approx e_{\mu}^{(i)}e_{\nu}^{(j)}\int d\beta_1 d\beta_2 d^2r_1 d^2r_2 \bar{\Psi}_{\gamma}^{(i)}\left(\beta_2,\vec{r}_2\right)\mathcal{A}^{d}\left(\beta_1,\vec{r}_1;\beta_2,\vec{r}_2;\Delta\right)\Psi_{\gamma}^{(j)}\left(\beta_1,\vec{r}_1\right), \tag{3}$$

where $e_{\mu}^{(i)}$ is the photon polarization vector; $\beta_{1,2}$ are the light-cone fractional momenta of the quark and antiquark, $\vec{r}_{1,2}$ are the transverse distances in the final and initial dipoles respectively; Δ is the momentum transfer in the Compton scattering, $\mathcal{A}^{d}(...)$ is the scattering amplitude for the dipole state which also implicitly depends on s, c.m. energy squared, and $\Psi_{\gamma}^{(i)}\left(\beta_2,\vec{r}_2\right)$ is the wavefunction of the photon in the polarization state i [33].

At high energies in the small angle approximation, $\Delta/\sqrt{s}\ll 1$, the quark separation and fractional momenta are preserved, so,

$$\mathcal{I}m\,\mathcal{A}^{d}\left(\beta_1,\vec{r}_1;\beta_2,\vec{r}_2;\Delta\right)\;\approx\;\delta\left(\beta_1-\beta_2\right)\delta\left(\vec{r}_1-\vec{r}_2\right)Im\,f_{\bar{q}q}^{N}(\vec{r}_1,\vec{\Delta},\beta_1). \tag{4}$$

Generally, the amplitude $f_{\bar{q}q}^{N}(...)$ is a nonperturbative object, with asymptotic behavior for small r controlled by pQCD [31]:

$$f_{\bar{q}q}^{N}(\vec{r},\vec{\Delta},\beta)\sim r^2,$$

up to slowly varying corrections $\sim\ln(r)$.

Calculation of the RCS differential cross section also involves the real part of scattering amplitude, whose relation to the imaginary part is quite straightforward. According to [35], if the limit $\lim\limits_{s\to\infty}\left(\frac{\mathcal{I}m\,f}{s^{\alpha}}\right)$ exists and is finite, then the real part and imaginary parts of the forward amplitude are related as

$$\mathcal{R}e\,f(\Delta=0)=s^{\alpha}\tan\left[\frac{\pi}{2}\left(\alpha-1+\frac{\partial}{\partial\ln s}\right)\right]\frac{\mathcal{I}m\,f(\Delta=0)}{s^{\alpha}}. \tag{5}$$

In the model under consideration the imaginary part of the forward dipole amplitude indeed has a power dependence on energy, $\mathcal{I}m\,f(\Delta=0)(s)\sim s^{\alpha}$, so (5) simplifies to

$$\frac{\mathcal{R}e\,\mathcal{A}}{\mathcal{I}m\,\mathcal{A}}\;=\tan\left(\tfrac{\pi}{2}(\alpha-1)\right)\equiv\epsilon. \tag{6}$$

This fixes the phase of the forward Compton amplitude, which we retain for nonzero momentum transfers assuming for the real and imaginary parts similar dependences on. Finally we arrive at,

$$\mathcal{A}_{\mu\nu}\approx(\epsilon+i)e_{\mu}^{(i)}(q')e_{\nu}^{(j)}(q)\int d^2r\int d\beta\,\bar{\Psi}_{\gamma}^{(i)}(\beta,r)\Psi_{\gamma}^{(j)}(\beta,r)\,Im\,f_{\bar{q}q}^{N}(\vec{r},\vec{\Delta},\beta,s), \tag{7}$$

For the cross-section of unpolarized Compton scattering, from (7) we obtain,

$$\begin{aligned}\frac{d\sigma_{el}^{\gamma p}}{dt}\;&=\;\frac{1+\epsilon^2}{16\pi}\sum_{ij}\left|\mathcal{A}_{\mu\nu}^{(ij)}\right|^2=\\&=\;\frac{1+\epsilon^2}{16\pi}\sum_{ij}\left|\int d^2r\int d\beta\,\bar{\Psi}_{\gamma}^{(i)}(\beta,r)\Psi_{\gamma}^{(j)}(\beta,r)\,Im\,f_{\bar{q}q}^{N}(\vec{r},\vec{\Delta},\beta)\right|^2.\end{aligned} \tag{8}$$

The imaginary part of the forward amplitude (7) gives the total photoabsorption cross-section,

$$\sigma_{tot}^{\gamma p}=\frac{1}{16\pi}\int d\beta d^2r\left|\Psi_{\gamma}(\beta,r)\right|^2 Im\,f_{\bar{q}q}^{N}\left(\vec{r},\vec{\Delta},\beta\right). \tag{9}$$

Formulas (8,9) are used further for numerical calculations.

III. WAVEFUNCTIONS FROM THE INSTANTON VACUUM

In this section we present briefly some details of the wavefunction evaluation in the instanton vacuum model (see [36, 37, 38] and references therein). The central object of the model is the partition function of the light quarks, which has the form

$$Z[v] = \int d\lambda \mathcal{D}\bar{\psi}\mathcal{D}\psi\mathcal{D}\Phi e^{iS[\lambda,v,\bar{\psi},\psi,\Phi]}, \tag{10}$$

where the effective action $S[\lambda, v, \bar{\psi}, \psi, \Phi]$ is defined as [38, 41]

$$S[\lambda, v, \bar{\psi}, \psi, \Phi] = \int d^4x \left(\frac{N}{V} \ln \lambda + 2\Phi^2(x) - \bar{\psi} \left(\hat{p} + \hat{v} - m - c\bar{L} f \otimes \Phi \cdot \Gamma_m \otimes fL \right) \psi \right).$$

Here ψ and Φ are the fields of constituent quarks and mesons respectively, N/V is the density of the instanton gas, $\hat{v} \equiv v_\mu \gamma^\mu$ is the external vector current corresponding to the photon, L is the gauge factor,

$$L(x, z) = P \exp \left(i \int_z^x d\zeta^\mu v_\mu(\zeta) \right), \tag{11}$$

which provides the gauge covariance of the action, and the nonlinear term in explicit form is

$$-c\bar{\psi}\bar{L}f \otimes \Phi \cdot \Gamma_m \otimes fL\psi \equiv -c \int d^4x d^4y d^4z \bar{\psi}(x)\bar{L}(x-z)\tilde{f}(x-z) \left(\sum_i \Phi_i(z)\Gamma_{m,i} \right) \tilde{f}(z-y)L(z-y)\psi(y) \tag{12}$$

where Γ_m is one of the matrices, $\Gamma_m = \{1, i\vec{\tau}, \gamma_5, i\vec{\tau}\gamma_5\}$, $\tilde{f}(x-y) = \int \frac{d^4p}{(2\pi)^4} f(p) e^{-ip\cdot(x-y)} f(p)$, and $f(p)$ is the Fourier transform of the zero-mode profile.

In the leading order in N_c, we have the same Feynman rules as in the perturbative theory, but with momentum-dependent quark mass $\mu(p)$ in the quark propagator

$$S(p) \;=\; \frac{1}{\hat{p} - \mu(p) + i0}. \tag{13}$$

The mass of the constituent quark has a form

$$\mu(p) = m + M\, f^2(p),$$

where $m \approx 5$ MeV is the current quark mass, $M \approx 350$ MeV is the dynamical mass generated by the interaction with the instanton vacuum background. Due to the presence of instantons the coupling of a vector current to a quark is also modified,

$$\begin{aligned} \hat{v} \;&\equiv\; v_\mu \gamma^\mu \to \hat{V} = \hat{v} + \hat{V}^{nonl}, \\ \hat{V}^{nonl} \;&\approx\; -2Mf(p)\frac{df(p)}{dp_\mu} v_\mu(q) + \mathcal{O}\left(q^2\right), \end{aligned} \tag{14}$$

where p is the momentum of the incoming quark, and q is the momentum of the photon. Notice that for an arbitrary photon momentum q the expression for $\hat{V}^{nonl}$ depends on the choice of the path in (11) and as a result one can find in the literature different expressions used for evaluations [33, 39, 40, 41]. In the limit $p \to \infty$ the function $f(p)$ falls off as $\sim \frac{1}{p^3}$, so for large $p \gg \rho^{-1}$, where $\rho \approx (600\, MeV)^{-1}$ is the mean instanton size, the mass of the quark $\mu(p) \approx m$ and vector current interaction vertex $\hat{V} \approx \hat{v}$. However we would like to emphasize that the wavefunction $\Psi(\beta, r)$ gets contribution from both the soft and the hard parts, so even in the large-Q limit the instanton vacuum function is different from the well-known perturbative result.

We have to evaluate the wavefunctions associated with the following matrix elements:

$$I_\Gamma(\beta, \vec{r}) \;=\; \int \frac{dz}{2\pi} e^{i\left(\beta + \frac{1}{2}\right)q\cdot z} \left\langle 0 \left| \bar{\psi}\left(-\frac{z}{2}n - \frac{\vec{r}}{2} \right) \Gamma \psi \left(\frac{z}{2}n + \frac{\vec{r}}{2} \right) \right| \gamma(q) \right\rangle, \tag{15}$$

where Γ is one of the matrices $\Gamma = \{\gamma_\mu, \gamma_\mu\gamma_5, \sigma_{\mu\nu}\}$. In the leading order in N_c one can easily obtain

$$I_\Gamma = \int \frac{d^4p}{(2\pi)^4} e^{i\vec{p}_\perp \vec{r}_\perp} \delta \left(p^+ - \left(\beta + \frac{1}{2} \right) q^+ \right) Tr \left(S(p)\hat{V}S(p+q)\Gamma \right). \tag{16}$$

The evaluation of (16) is quite tedious but straightforward. Details of this evaluation may be found in [33].

The overlap of the initial and final photon wavefunctions in (8) was evaluated according to

$$\Psi^{(i)*}(\beta,r,Q^2=0)\Psi^{(i)}(\beta,r,Q^2)=\sum_\Gamma I^*_\Gamma\left(\beta,r^*,0\right)I_\Gamma\left(\beta,r,Q^2\right), \tag{17}$$

where summation is done over possible polarization states $\Gamma=\{\gamma_\mu,\gamma_\mu\gamma_5,\sigma_{\mu\nu}\}$. In the final state we should use $r^*_\mu=r_\mu+n_\mu\frac{q'_\perp\cdot r_\perp}{q_+}=r_\mu-n_\mu\frac{\Delta_\perp\cdot r_\perp}{q_+}$, which is related to the reference frame with $q'_{\perp,\mu}=0$ in which the components (16) were evaluated.

IV. NUMERICAL RESULTS

A. Photoabsorption

The Bjorken variable used in DIS, $x=Q^2/\left(2\,p\cdot q\right)$, is not appropriate at small photon virtualities, since it does not have the meaning of a fractional quark momentum any more, and may be very small even at low energies. In particular, for RCS the Bjorken variable x defined in this way would be zero. Therefore, one should rely on the phenomenological dipole cross section which depends on energy, rather than x. We use the s-dependent dipole cross section proposed in [42], which saturates at large separations in analogy to the x-dependent one proposed in [43]. Correspondingly, for the elastic dipole amplitude we employ the model developed in [34, 44, 45, 46],

$$\begin{aligned} Im\,f^N_{\bar qq}(\vec r,\vec\Delta,\beta,s) &= \frac{\sigma_0(s)}{4}\exp\left[-\left(\frac{B(s)}{2}+\frac{R_0^2(s)}{16}\right)\vec\Delta^2_\perp\right]\times \\ &\times\left(e^{-i\beta\vec r\cdot\vec\Delta}+e^{i(1-\beta)\vec r\cdot\vec\Delta}-2e^{i\left(\frac12-\beta\right)\vec r\cdot\vec\Delta}e^{-\frac{r^2}{R_0^2(s)}}\right), \end{aligned} \tag{18}$$

where $\sigma_0(s)$, $R_0^2(s)$, $B(s)$ are the phenomenological parameters known from DIS and πp scattering data.

We employ the s-dependent parametrization of the dipole cross section suitable for soft processes [42]

$$\sigma_{\bar qq}(r,s) = \sigma_0(s)\left(1-e^{-r^2/R_0^2(s)}\right), \tag{19}$$

$$\sigma_0(s) = \sigma_{\pi p}(s)\left(1+\frac38\frac{R_0^2(s)}{r_\pi^2}\right), \tag{20}$$

$$R_0(s) = 0.88\,fm\times\left(\frac{s_0}{s}\right)^{0.14}, \tag{21}$$

where $s_0\approx1000\,GeV^2$. For the pion cross section we use the parametrization and fit of [47], namely its Pomeron part,

$$\sigma_{\pi p}(s)=23.6\left(\frac{s}{s_0}\right)^{0.079}mb. \tag{22}$$

The parameter $B(s)$ in Eq. (18), is related to the t-slope of the differential cross section of elastic πp scattering [44, 45, 46],

$$B(s)=B^{\pi p}_{el}(s)-\frac13\left\langle r^2_{ch}\right\rangle_\pi-\frac18R_0^2(s) \tag{23}$$

Here we rely on the Regge factorization and use $B^{\pi p}_{el}(s)=B_0+2\alpha'_P(0)\ln\left(s/\mu_0^2\right)$, with $B_0=6$ GeV^{-2}, $\left\langle r^2_{ch}\right\rangle_\pi=0.44$ fm^2,$\alpha'_P(0)=0.25$ GeV^{-2}, and $\mu_0=1$ GeV.

This parametrization may be used in Eqs. (8-9) only at very high energies where in terms of the Regge theory, the Pomeron term in the cross section dominates. So far only two data points shown in Fig. 1 are available for $\sigma_{\gamma p}$ from the H1 and ZEUS experiments [48], and our parameter free calculation agrees well with these data.

In order to extend the model down to smaller values of $\sqrt{s}$, where more data are available, we added the Reggeon contribution, which was fitted to the photoabsorption data in [47]

$$\sigma^{(R)}_{\gamma p}(s)=129\,nb\times s^{-0.4525}. \tag{24}$$

Besides, the Pomeron part of the dipole cross section parametrized as in Eqs. (19-21) exposes some problems at low energies. Indeed, as one can see from (21), the saturation radius $R_0(s)$ grows and may substantially exceed the confinement radius. In order to regularize the low-energy behavior of $R_0(s)$, we modify Eq. (21) as follows,

$$R_0(s) \Rightarrow \tilde{R}_0(s) = 0.88\, fm \left(\frac{s_0}{s+s_1}\right)^{0.14} . \tag{25}$$

Fit to low-energy photoabsorption data allows to fix this parameter at $\sqrt{s_1} = 60$ GeV (see Fig. (1) for more details). Since further evaluations are done in the LHC energy range, the difference between (21) and (25) is negligible, as one can see from Fig. (1). Indeed, both parameterizations coincide for $\sqrt{s} \gtrsim 10$ GeV. In the right pane of the Fig. (1) the contributions of the color dipole (9) and Reggeon (24) terms are displayed separately.

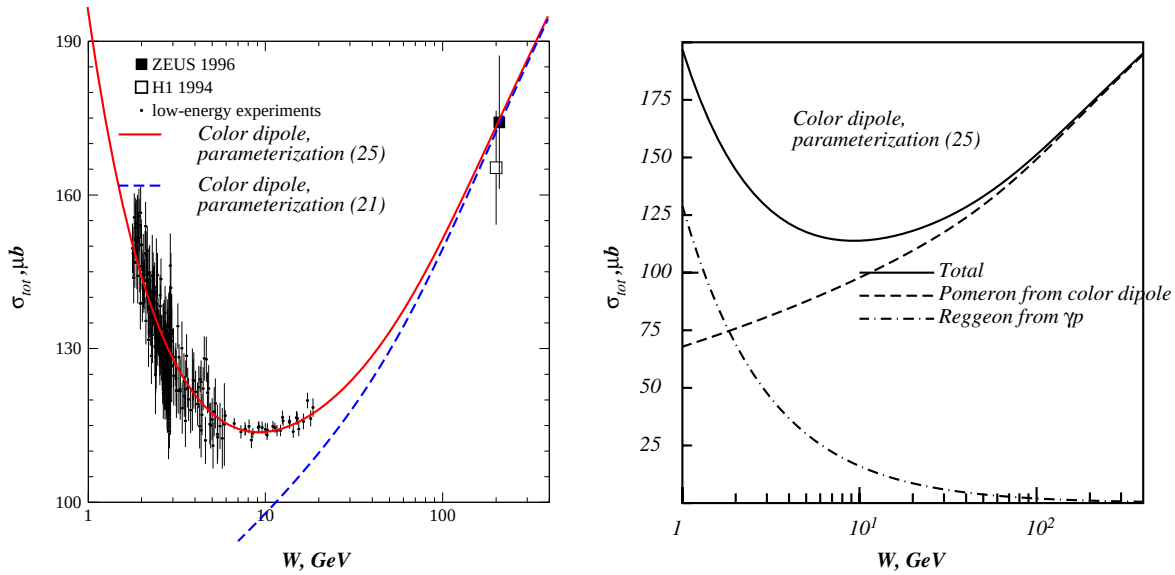

FIG. 1: [Color online] Photoabsorption cross-section in the color dipole model as function of c.m. energy, $W = \sqrt{s}$. Left: comparison of calculations with experimental data from ZEUS [48]. Dashed line corresponds to the parameterization (19-21), solid line corresponds to addition of the Reggeon term,Eq. (25). Right: the contributions of the Pomeron and Reggeon parts plotted separately. At $W \gtrsim 10$ GeV the Reggeon contribution becomes negligibly small.

B. Compton scattering

Using parameterization (19-22), we calculate the elastic RCS differential cross-section as

$$\frac{d\sigma_{el}^{\gamma p}}{dt} = \frac{1+\epsilon^2}{16\pi} \sum_{ij} \left| \int d^2r \int d\beta\, \bar{\Psi}_\gamma^{(i)}(\beta,r)\Psi_\gamma^{(j)}(\beta,r)\, Im\, f_{\bar{q}q}^N(\vec{r},\vec{\Delta},\beta) + 16\pi\sigma_{\gamma p}^{(I\!R)}(s) e^{B_{I\!R}(s)t} \right|^2 . \tag{26}$$

Since extraction of reggeon parameters from experimental data yields huge uncertainties [52], in this paper we rely on the f-dominance of the pomeron [53] and take the reggeon slope as

$$B_{I\!R}(s) = B_1 + 2\alpha'_{I\!R}(0) \ln\left(\frac{s}{\mu_0^2}\right), \tag{27}$$

where $B_1 = B_0 = 6$ GeV^{-2}, $\alpha'_{I\!R}(0) = 0.9$ GeV^{-2}, and the results for the differential cross-section are presented in the Figure 2. As one can see from the left pane, for $s \gtrsim 10$ GeV^2 the cross-section rises with energy for small $|t|$, but falls at $|t| = 1$GeV^2. This corresponds to the Regge predicted energy dependence $s^{2(\alpha(t)-1)}$. However, a word of caution is in order here, since the linear t-dependence of the Pomeron trajectory may not continue at large $|t|$, and indeed data indicate that $\alpha_P(t)$ levels off [49]. On the right pane of the Figure 2 our predictions for the t-dependence of the cross

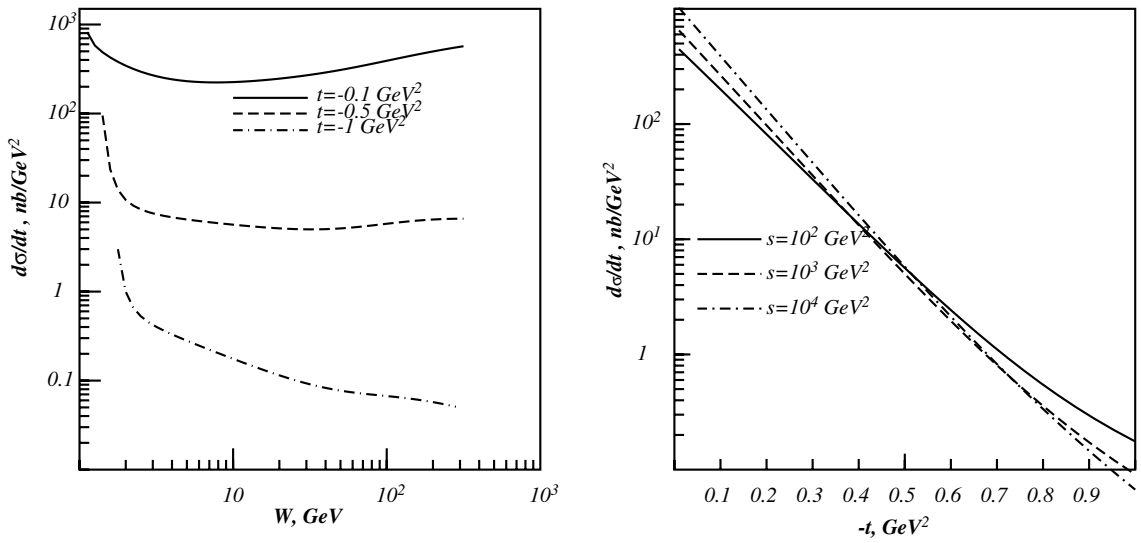

FIG. 2: RCS cross-section in the color dipole model. Left: Energy dependence of the RCS cross-section for different t, $W \equiv \sqrt{s_{\gamma p}}$. For $s \gtrsim 10$ GeV^2 the cross-section depends on the energy s approximately as $s^{2(\alpha(t)-1)}$. For $s \lesssim 10$ GeV^2 we have "soft" regime where contributions of reggeons dominate. Right: t-dependence of the RCS cross-section for different energies in the energy range of ultraperipheral collisions at LHC .

section are plotted for different energies. The cross section demonstrates a shrinkage of diffraction cone with energy in accordance with the Regge theory.

The RCS cross-section has been measured so far only at Jefferson Lab (JLAB) at energies $s \lesssim 10\,GeV^2$ [50]. In Figure 3 we compare predictions of the color dipole model with experimental data. Since these data also have relatively large $|t| \gtrsim 2$ GeV^2 (wide-angle Compton scattering), calculations in the dipole approach go beyond the kinematics of validity of the model. Indeed, Eqn. (18), lead to the RCS cross-section which decreases exponentially at fixed s/t, while the general pQCD analysis [51] predicts $1/s^6$ behavior.

As was discussed in the introduction, there are two approaches which are used to describe the wide-angle Compton scattering. The first one is valid for large $\Delta_\perp$[18, 19] and expresses the amplitude via the distribution amplitude of three valence quarks in the proton. The RCS cross-section in this approach was studied in [16, 17] and it was found that evaluation with widely used distribution amplitudes also underestimates the JLAB data [50]. Another description expresses the RCS amplitude via the $1/x$ moment of GPDs at zero skewedness, $\int \frac{dx}{x} H(x,0,t)$ [5, 20, 21]. This approach is able to describe the existing JLAB data. However the t-dependence of the cross-section in this approach depends on the model for the GPD used in the evaluation.

Since the experimental counting rate also includes the flux of quasi-real photons, we present in Fig. 4 the two-dimensional product of the flux and the differential RCS cross section,

$$\frac{d^2\sigma_{pp\to pp\gamma}}{dkdt} = \frac{dN_\gamma}{dk}\frac{d\sigma_{\gamma p\to\gamma p}}{dt}, \tag{28}$$

where k is the absolute value of the wave vector of the quasireal photon, and photon flux $\frac{dN_\gamma}{dk}$ is given, e.g., in [30].

V. SUMMARY

In this paper we evaluated the photoabsorption and RCS cross-sections within the color dipole model. We employed a photon wave function calculated in the instanton-vacuum model and incorporating nonperturbative effects [33]. For the dipole cross section we relied on an energy dependent parametrization, because Bjorken x is not a proper variable at low photon virtualities.

We found that the model describes available data for the photoabsorption cross section from the ZEUS and H1 data quite well, justifying application of the color dipole for processes with real photons. Applicability of the dipole model was extended down to smaller energies, $\sqrt{s} \lesssim 30$ GeV, by freezing the saturation radius $R_s(s)$ Eq. (21) for the energy dependent parametrization [42], to make sure that it does not exceed the confinement radius.

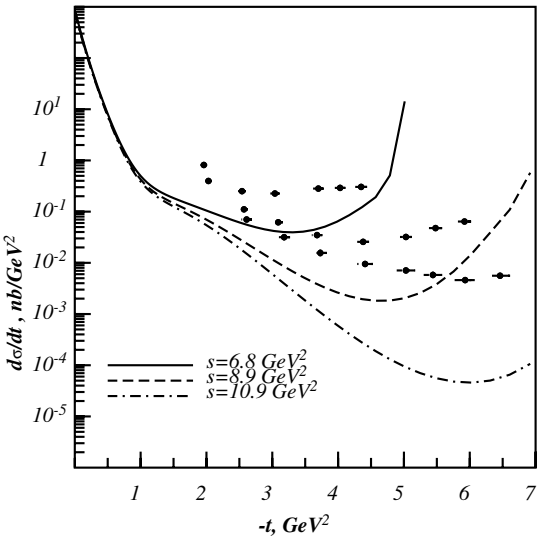

FIG. 3: Comparison of the RCS cross-section evaluated in the color dipole model with low-energy (large-angle) experimental data from JLAB [50].

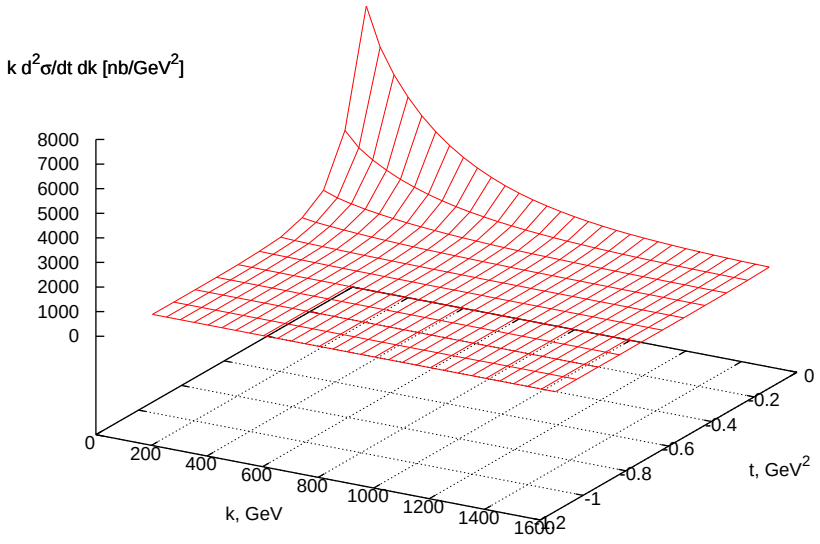

FIG. 4: [Color online] Twofold cross-section $kd^2\sigma/dtdk$

We also evaluated the RCS cross-sections and made predictions for the energy range to be accessed in ultra-peripheral collisions at LHC (Figure 2).

Acknowlegments

This work was supported in part by Fondecyt (Chile) grants 1090291, 1090073 , and by DFG (Germany) grant PI182/3-1.

---

[1] D. Mueller, D. Robaschik, B. Geyer, F. M. Dittes and J. Horejsi, Fortsch. Phys. **42**, 101 (1994) [arXiv:hep-ph/9812448].
[2] X. D. Ji, Phys. Rev. D **55**, 7114 (1997).
[3] X. D. Ji, J. Phys. G **24**, 1181 (1998) [arXiv:hep-ph/9807358].
[4] A. V. Radyushkin, Phys. Lett. B **380**, 417 (1996) [arXiv:hep-ph/9604317].
[5] A. V. Radyushkin, Phys. Rev. D **56**, 5524 (1997).
[6] A. V. Radyushkin, arXiv:hep-ph/0101225.
[7] X. D. Ji and J. Osborne, Phys. Rev. D **58** (1998) 094018 [arXiv:hep-ph/9801260].
[8] J. C. Collins and A. Freund, Phys. Rev. D **59** (1999) 074009 [arXiv:hep-ph/9801262].
[9] J. C. Collins, L. Frankfurt and M. Strikman, Phys. Rev. D **56**, 2982 (1997).
[10] S. J. Brodsky, L. Frankfurt, J. F. Gunion, A. H. Mueller and M. Strikman, Phys. Rev. D **50**, 3134 (1994).
[11] K. Goeke, M. V. Polyakov and M. Vanderhaeghen, Prog. Part. Nucl. Phys. **47**, 401 (2001) [arXiv:hep-ph/0106012].
[12] M. Diehl, T. Feldmann, R. Jakob and P. Kroll, Nucl. Phys. B **596**, 33 (2001) [Erratum-ibid. B **605**, 647 (2001)] [arXiv:hep-ph/0009255].
[13] A. V. Belitsky, D. Mueller and A. Kirchner, Nucl. Phys. B **629**, 323 (2002) [arXiv:hep-ph/0112108].
[14] M. Diehl, Phys. Rept. **388**, 41 (2003) [arXiv:hep-ph/0307382].
[15] A. V. Belitsky and A. V. Radyushkin, Phys. Rept. **418**, 1 (2005) [arXiv:hep-ph/0504030].
[16] A. S. Kronfeld and B. Nizic, Phys. Rev. D **44** (1991) 3445 [Erratum-ibid. D **46** (1992) 2272].
[17] T. C. Brooks and L. J. Dixon, Phys. Rev. D **62** (2000) 114021 [arXiv:hep-ph/0004143].
[18] G. P. Lepage and S. J. Brodsky, Phys. Lett. B **87** (1979) 359.
[19] G. P. Lepage and S. J. Brodsky, Phys. Rev. D **22** (1980) 2157.
[20] M. Diehl, T. Feldmann, R. Jakob and P. Kroll, Eur. Phys. J. C **8** (1999) 409 [arXiv:hep-ph/9811253].
[21] M. Diehl, T. Feldmann, R. Jakob and P. Kroll, Eur. Phys. J. C **39** (2005) 1 [arXiv:hep-ph/0408173].
[22] M. Klein and P. Newman, CERN Cour. **49N3** (2009) 22.
[23] LHEC website `http://www.ep.ph.bham.ac.uk/exp/LHeC/`
[24] EIC website `http://www.phenix.bnl.gov/WWW/publish/abhay/Home_of_EIC/`
[25] EIC White paper `http://www.phenix.bnl.gov/WWW/publish/abhay/Home_of_EIC/NSAC2007/070424_EIC.pdf`
[26] B. I. Abelev *et al.* [STAR Collaboration], Phys. Rev. C **77** (2008) 034910 [arXiv:0712.3320 [nucl-ex]].
[27] J. Adams *et al.* [STAR Collaboration], Phys. Rev. C **70** (2004) 031902 [arXiv:nucl-ex/0404012].
[28] C. Adler *et al.* [STAR Collaboration], Phys. Rev. Lett. **89** (2002) 272302 [arXiv:nucl-ex/0206004].
[29] D. G. d'Enterria, arXiv:nucl-ex/0601001.
[30] K. Hencken *et al.*, Phys. Rept. **458** (2008) 1 [arXiv:0706.3356 [nucl-ex]].
[31] B. Z. Kopeliovich, L. I. Lapidus and A. B. Zamolodchikov, JETP Lett. **33** (1981) 595 [Pisma Zh. Eksp. Teor. Fiz. **33** (1981) 612].
[32] A. H. Mueller, Nucl. Phys. B **335**, 115 (1990); A. H. Mueller and B. Patel, Nucl. Phys. B **425**, 471 (1994) [arXiv:hep-ph/9403256].
[33] A. E. Dorokhov, W. Broniowski and E. Ruiz Arriola, Phys. Rev. D **74** (2006) 054023 [arXiv:hep-ph/0607171].
[34] B. Z. Kopeliovich, I. Schmidt and M. Siddikov, Phys. Rev. D **79** (2009) 034019 [arXiv:0812.3992 [hep-ph]].
[35] J. B. Bronzan, G. L. Kane and U. P. Sukhatme, Phys. Lett. B **49** (1974) 272.
[36] T. Schafer and E. V. Shuryak, Rev. Mod. Phys. **70** (1998) 323 [arXiv:hep-ph/9610451].
[37] D. Diakonov and V. Y. Petrov, Nucl. Phys. B **272** (1986) 457
[38] D. Diakonov, M. V. Polyakov and C. Weiss, Nucl. Phys. B **461** (1996) 539 [arXiv:hep-ph/9510232].
[39] I. V. Anikin, A. E. Dorokhov and L. Tomio, Phys. Part. Nucl. **31** (2000) 509 [Fiz. Elem. Chast. Atom. Yadra **31** (2000) 1023].
[40] A. E. Dorokhov and W. Broniowski, Eur. Phys. J. C **32** (2003) 79 [arXiv:hep-ph/0305037].
[41] K. Goeke, M. M. Musakhanov and M. Siddikov, Phys. Rev. D **76** (2007) 076007 [arXiv:0707.1997 [hep-ph]]
[42] B.Z. Kopeliovich, A. Schfer and A.V. Tarasov, Phys. Rev. D**62**, 054022 (2000).
[43] K. J. Golec-Biernat and M. Wusthoff, Phys. Rev. D **59** (1999) 014017 [arXiv:hep-ph/9807513].
[44] B. Z. Kopeliovich, H. J. Pirner, A. H. Rezaeian and I. Schmidt, Phys. Rev. D **77** (2008) 034011 [arXiv:0711.3010 [hep-ph]].
[45] B. Z. Kopeliovich, A. H. Rezaeian and I. Schmidt, arXiv:0809.4327 [hep-ph], to appear in Phys. Rev. D.
[46] B. Z. Kopeliovich, I. K. Potashnikova, I. Schmidt and J. Soffer, arXiv:0805.4534 [hep-ph].
[47] A. Donnachie and P. V. Landshoff, Phys. Lett. B **296** (1992) 227 [arXiv:hep-ph/9209205].
[48] S. Chekanov *et al.* [ZEUS Collaboration], Nucl. Phys. B **627** (2002) 3 [arXiv:hep-ex/0202034].
[49] A. Brandt *et al.* [UA8 Collaboration], Nucl. Phys. B **514** (1998) 3 [arXiv:hep-ex/9710004].
[50] A. Danagoulian *et al.* [Hall A Collaboration], Phys. Rev. Lett. **98** (2007) 152001 [arXiv:nucl-ex/0701068].
[51] S. J. Brodsky and G. R. Farrar, Phys. Rev. Lett. **31** (1973) 1153.

[52] A. Aktas *et al.* [H1 Collaboration], Eur. Phys. J. C **48** (2006) 749 [arXiv:hep-ex/0606003].
[53] A. C. Irving, Nucl. Phys. B **121**, 176 (1977).